X-Band Radar Simulation

Complete Technical Documentation

From Ray Tracing to PPI Display

Radar Simulation Framework

January 9, 2026

Contents

1 System Overview

This document provides a complete technical description of the X-band radar simulation software, covering every stage from 3D world construction to final PPI display rendering.

1.1 High-Level Pipeline

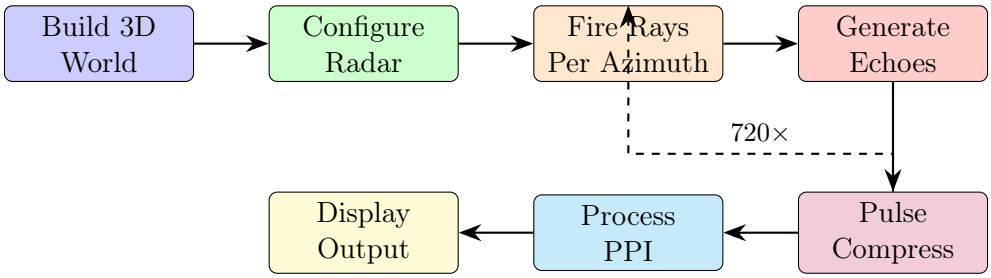

Figure 1: High-level simulation pipeline. The ray-to-compress loop executes 720 times (once per azimuth).

1.2 Key Parameters

Parameter	Value	Derived From
Center Frequency	$f_0 = 9.41$ GHz	X-band marine radar
Wavelength	$\lambda = 3.19$ cm	$\lambda = c/f_0$
Bandwidth	$B = 50$ MHz	Chirp sweep
Pulse Width	$T = 10$ μs	Waveform design
Range Resolution	$\Delta R = 3.0$ m	$\Delta R = c/(2B)$
Beamwidth (H)	$\theta_{3dB} = 3.9$	Antenna aperture
Azimuths	720	0.5° spacing
Rays per Azimuth	2000	Monte Carlo sampling

Table 1: Primary simulation parameters

2 Stage 1: 3D World Construction

2.1 Scene Geometry

The simulation world is constructed from triangle meshes. Each target is defined by vertices and faces, positioned at specific coordinates.

2.2 Triangle Mesh Representation

Every 3D object is decomposed into triangles:

3 Stage 2: Radar Configuration

3.1 Frequency and Wavelength

The radar operates at X-band:

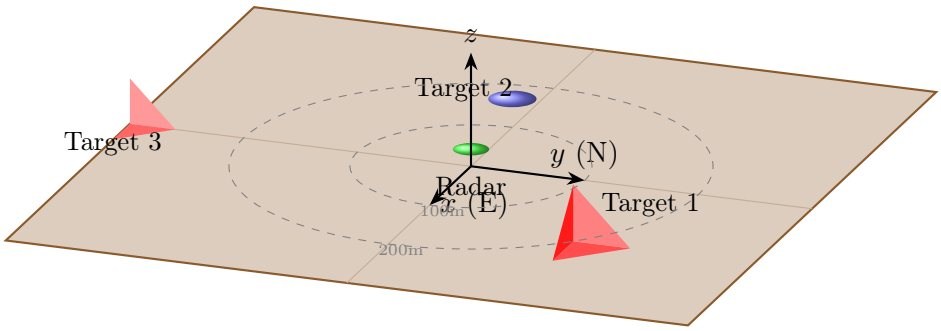

Figure 2: 3D scene with radar at origin and multiple targets. Ground plane shown in brown. Range rings indicate distance from radar.

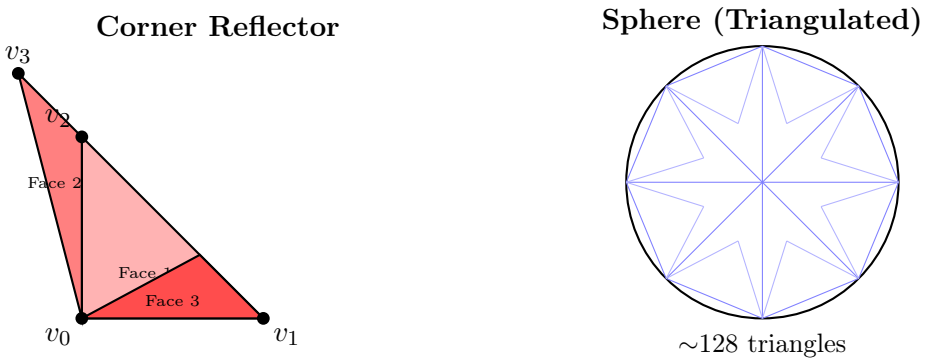

Figure 3: Objects represented as triangle meshes. Left: Corner reflector (3 triangles). Right: Sphere approximated by icosphere subdivision.

$$\lambda = \frac{c}{f_0} = \frac{2.998 \times 10^8 \text{ m/s}}{9.41 \times 10^9 \text{ Hz}} = 0.0319 \text{ m} = 3.19 \text{ cm} \tag{1}$$

3.2 Antenna Pattern

The antenna gain pattern follows a sinc-squared approximation:

$$G(\theta) = G_0 \left[\frac{\sin(\pi u)}{\pi u} \right]^2, \quad u = \frac{2.783 \cdot \theta}{\theta_{3dB}} \tag{2}$$

3.3 Two-Way Pattern

For monostatic radar (same antenna for TX and RX), the two-way pattern is:

$$G_{2-way}(\theta_{az}, \theta_{el}) = [G(\theta_{az}) \cdot G(\theta_{el})]^2 \tag{3}$$

This fourth-power relationship means the effective beamwidth is narrower than the one-way pattern.

4 Stage 3: Ray Tracing

4.1 Ray Generation

For each azimuth pointing direction, we generate 2000 rays distributed within the antenna beam:

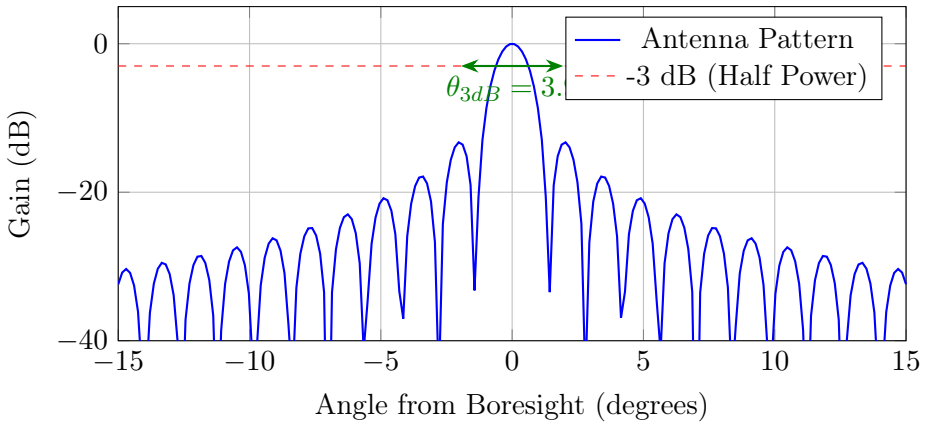

Figure 4: Antenna gain pattern showing main lobe and sidelobes. The 3 dB beamwidth defines angular resolution.

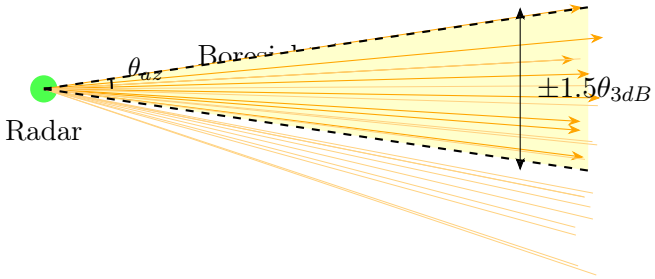

Figure 5: Ray generation for a single azimuth. 2000 rays are distributed randomly within $\pm 1.5\times$ beamwidth of boresight. Orange arrows show individual rays.

4.2 Ray Direction Calculation

Each ray direction is computed from azimuth and elevation offsets:

$$\phi_{ray} = \phi_{boresight} + \Delta\phi, \quad \Delta\phi \sim \mathcal{U}(-1.5\theta_{az}, +1.5\theta_{az}) \tag{4}$$

$$\theta_{ray} = \Delta\theta, \quad \Delta\theta \sim \mathcal{U}(-1.5\theta_{el}, +1.5\theta_{el}) \tag{5}$$

The unit direction vector is:

$$\hat{d} = \begin{pmatrix} \cos(\theta_{ray})\cos(\phi_{ray}) \\ \cos(\theta_{ray})\sin(\phi_{ray}) \\ \sin(\theta_{ray}) \end{pmatrix} \tag{6}$$

4.3 Ray-Triangle Intersection

We use the Möller-Trumbore algorithm to find where each ray intersects scene triangles.

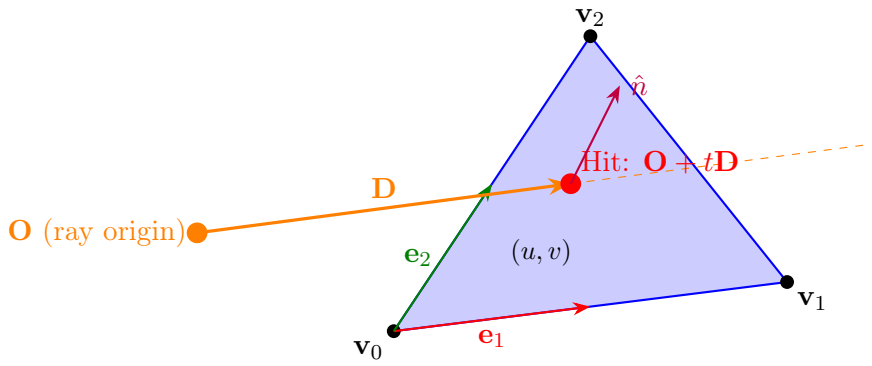

Figure 6: Ray-triangle intersection. The ray from origin $\mathbf{O}$ in direction $\mathbf{D}$ intersects the triangle at parameter t. Barycentric coordinates (u, v) determine if the hit is inside the triangle.

4.3.1 Möller-Trumbore Algorithm

Algorithm 1 Ray-Triangle Intersection

$\mathbf{e}_1 \leftarrow \mathbf{v}_1 - \mathbf{v}_0$ ▷ Edge vectors
$\mathbf{e}_2 \leftarrow \mathbf{v}_2 - \mathbf{v}_0$
$\mathbf{h} \leftarrow \mathbf{D} \times \mathbf{e}_2$
$a \leftarrow \mathbf{e}_1 \cdot \mathbf{h}$
if $|a| < \epsilon$ **then**
    return no intersection ▷ Ray parallel to triangle
end if
$f \leftarrow 1/a$
$\mathbf{s} \leftarrow \mathbf{O} - \mathbf{v}_0$
$u \leftarrow f \cdot (\mathbf{s} \cdot \mathbf{h})$
if $u < 0$ or $u > 1$ **then**
    return no intersection
end if
$\mathbf{q} \leftarrow \mathbf{s} \times \mathbf{e}_1$
$v \leftarrow f \cdot (\mathbf{D} \cdot \mathbf{q})$
if $v < 0$ or $u + v > 1$ **then**
    return no intersection
end if
$t \leftarrow f \cdot (\mathbf{e}_2 \cdot \mathbf{q})$
if $t > \epsilon$ **then**
    return intersection at distance t
end if

5 Stage 4: Echo Signal Generation

For each ray that hits a target, we generate an echo signal. This is the physics-critical stage.

5.1 LFM Chirp Waveform

The transmitted waveform is a Linear Frequency Modulated (LFM) chirp:

$$s_{TX}(t) = \exp\left(j\pi K t^2\right), \quad K = \frac{B}{T} = \frac{50 \times 10^6}{10 \times 10^{-6}} = 5 \times 10^{12} \text{ Hz/s} \tag{7}$$

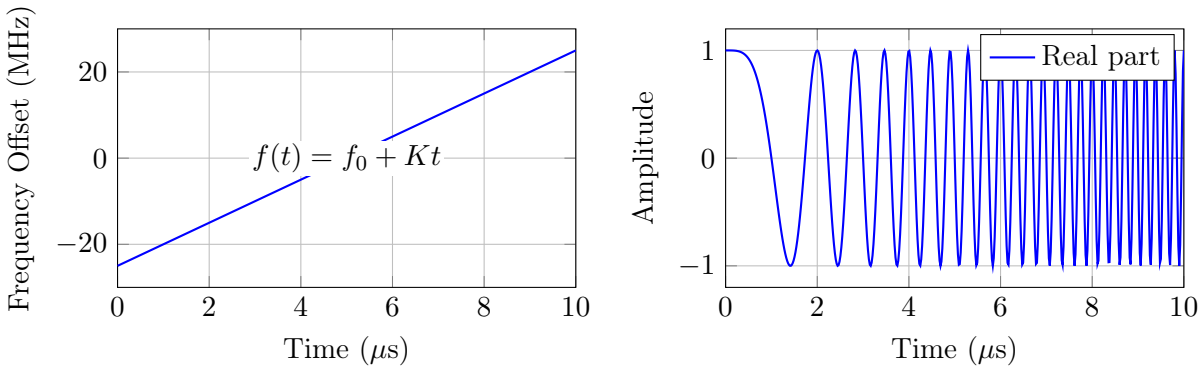

(a) Instantaneous frequency vs time

(b) Real part of chirp signal

Figure 7: LFM chirp waveform. Left: Frequency increases linearly from $-B/2$ to $+B/2$. Right: The resulting oscillation with increasing frequency.

5.2 Single Echo Generation

For a ray hitting at range R:

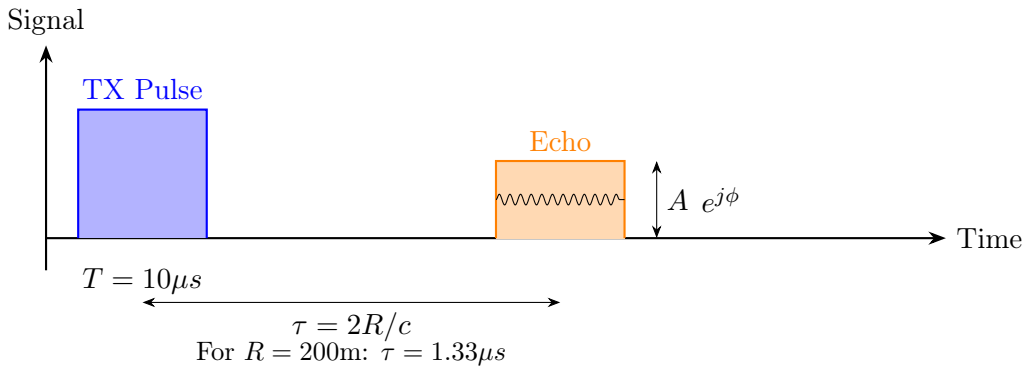

Figure 8: Echo timing. The echo arrives after round-trip delay $\tau = 2R/c$ with amplitude A and phase ϕ.

5.2.1 Amplitude Calculation

The echo amplitude includes multiple factors:

$$A = \underbrace{G_{2way}(\theta_{az}, \theta_{el})}_{\text{Antenna Pattern}} \cdot \underbrace{\frac{1}{R^2 + 1}}_{\text{Path Loss}} \cdot \underbrace{L_{atm}(R)}_{\text{Atmospheric}} \cdot \underbrace{|F|^2}_{\text{Multipath}} \tag{8}$$

Antenna Pattern Weighting Each ray has an offset from boresight. The antenna gain at that offset determines how much power goes in that direction:

$$G_{2way} = \left[\text{sinc}^2\left(\frac{2.783 \cdot \Delta\phi}{\theta_{az}}\right) \cdot \text{sinc}^2\left(\frac{2.783 \cdot \Delta\theta}{\theta_{el}}\right)\right]^2 \tag{9}$$

Atmospheric Attenuation At X-band, atmospheric gases absorb some energy:

$$L_{atm}(R) = 10^{-\gamma_{dB} \cdot 2R/(10 \cdot 1000)} \tag{10}$$

where $\gamma_{dB} \approx 0.01$ dB/km combines oxygen and water vapor absorption.

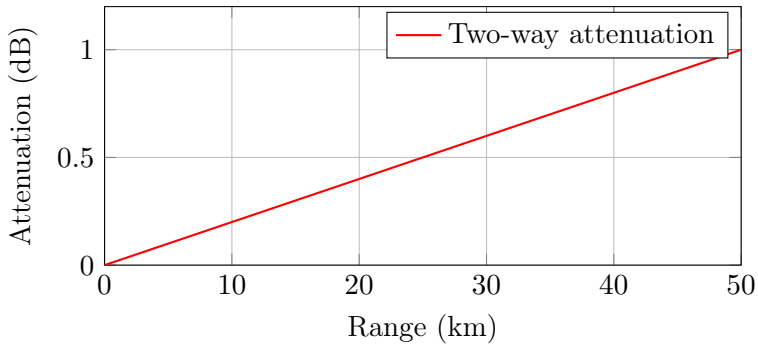

Figure 9: Atmospheric attenuation vs range at X-band. At 50 km, two-way loss is about 1 dB.

5.2.2 Phase Calculation

The phase accumulates over the round-trip path:

$$\phi = \frac{4\pi f_0 R}{c} = \frac{4\pi R}{\lambda} \tag{11}$$

Key insight: A range change of $\lambda/2 = 1.6$ cm causes a phase shift of 2π (360°).

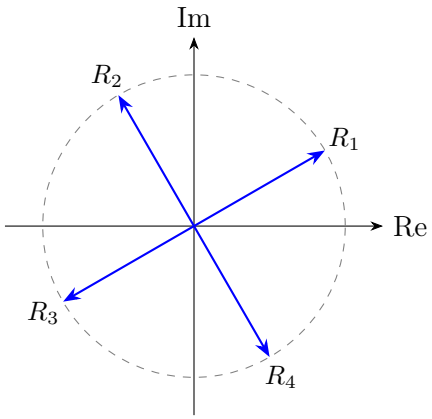

Figure 10: Phasor representation of echoes at different ranges. The phase rotates rapidly with range due to the short wavelength.

5.3 Multipath: Two-Ray Model

When a target is above a reflective surface, two paths exist:

The multipath propagation factor is:

$$F = 1 + \Gamma \cdot \rho_s \cdot D \cdot e^{-jk\Delta R} \cdot \frac{R_d}{R_1 + R_2} \tag{12}$$

where:

- Γ = Fresnel reflection coefficient (complex, depends on polarization)
- ρ_s = Roughness factor (reduces specular reflection)
- D = Divergence factor (spherical Earth effect)
- $k = 2\pi/\lambda$ = Wavenumber

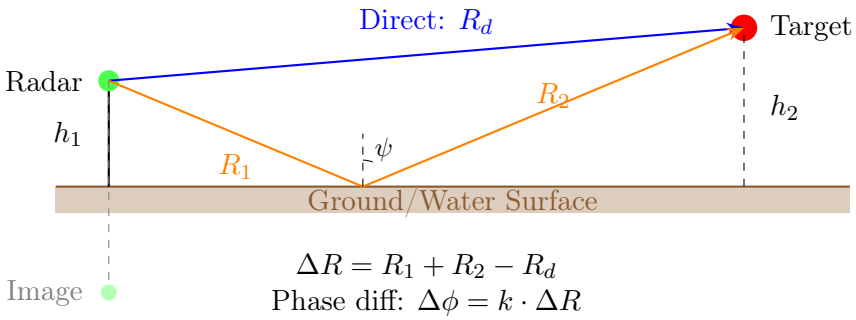

Figure 11: Two-ray multipath geometry. The direct path interferes with the ground-reflected path, causing constructive or destructive interference depending on path difference.

5.4 Complete Echo Signal

For hit i at range R_i:

$$\text{echo}_i(t) = A_i \cdot e^{j\phi_i} \cdot s_{TX}(t) \tag{13}$$

Added to received signal at the correct delay:

$$s_{RX}(t) = \sum_{i=1}^{N_{hits}} \text{echo}_i\left(t - \frac{2R_i}{c}\right) \tag{14}$$

6 Stage 5: Pulse Compression

6.1 The Matched Filter

Pulse compression correlates the received signal with the transmitted waveform:

$$s_{compressed}(t) = s_{RX}(t) \star s_{TX}^*(-t) = \mathcal{F}^{-1}\left\{S_{RX}(f) \cdot S_{TX}^*(f)\right\} \tag{15}$$

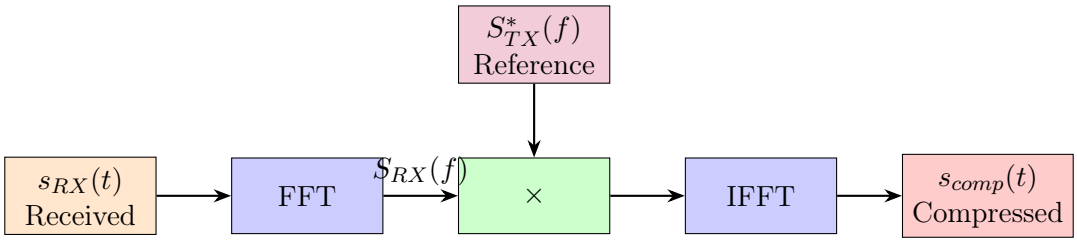

Figure 12: FFT-based matched filter implementation. Correlation in time domain equals multiplication in frequency domain.

6.2 Compression Result

The matched filter output for an LFM chirp is a sinc function:

$$|s_{compressed}(\tau)| \propto |\text{sinc}(B \cdot \tau)| \tag{16}$$

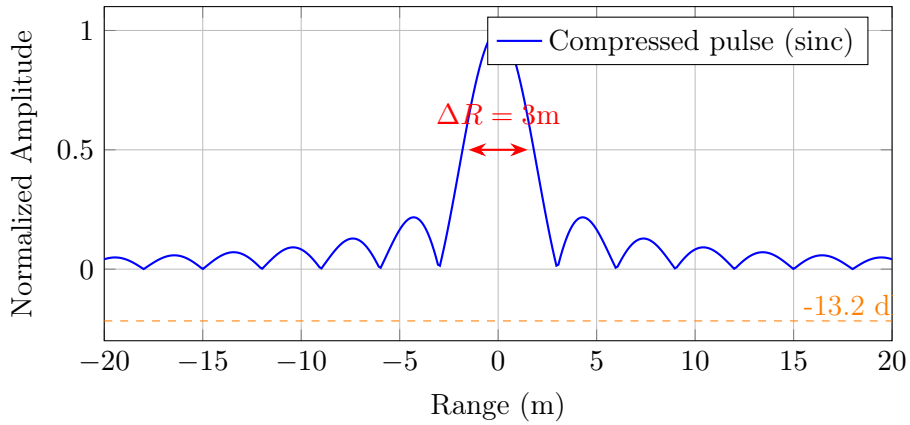

Figure 13: Matched filter output showing sinc function. Main lobe width equals range resolution. First sidelobe at -13.2 dB without windowing.

6.3 Windowing for Sidelobe Reduction

Applying a Hamming window to the reference waveform reduces sidelobes at the cost of slightly wider main lobe:

$$w(n) = 0.54 - 0.46 \cos\left(\frac{2\pi n}{N-1}\right) \tag{17}$$

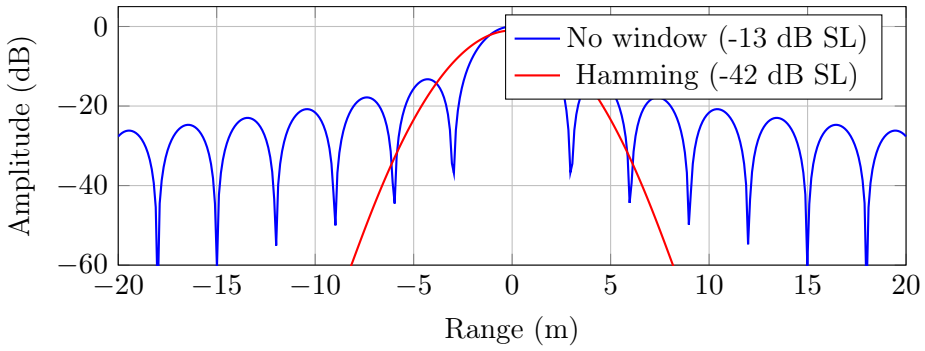

Figure 14: Effect of windowing on pulse compression. Hamming window reduces sidelobes from -13 dB to -42 dB.

7 Stage 6: PPI Processing

After running the simulation for all 720 azimuths, we have a raw PPI:

$$\text{PPI}_{raw}[\phi, R] = |s_{compressed}|^2, \quad \phi \in [0, 359.5], \quad R \in [0, R_{max}] \tag{18}$$

This shows **ray artifacts**—targets appear as thin radial lines because each ray deposits energy in only one azimuth bin.

7.1 Beam Spreading (Azimuth Convolution)

Real targets are illuminated for the entire time the beam sweeps past them. We simulate this by convolving along azimuth:

$$\text{PPI}_{spread}[\phi, R] = \text{PPI}_{raw}[\phi, R] \star_\phi g(\phi) \tag{19}$$

where $g(\phi)$ is a Gaussian kernel with $\sigma = \theta_{3dB}/2.355$:

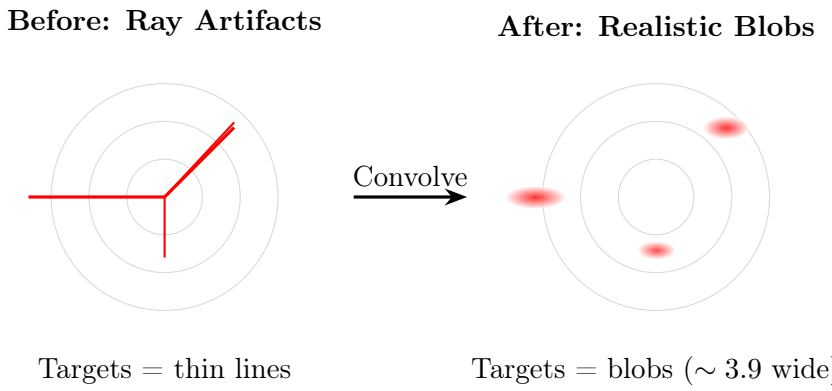

Figure 15: Effect of beam spreading convolution. Thin radial artifacts become realistic blob-shaped returns matching the antenna beamwidth.

7.2 2D Point Spread Function

A complete radar PSF spreads energy in both range and azimuth:

$$\text{PSF}(R, \phi) = \underbrace{\text{sinc}^2\left(\frac{R}{\Delta R}\right)}_{\text{Range (matched filter)}} \cdot \underbrace{\exp\left(-\frac{\phi^2}{2\sigma_\phi^2}\right)}_{\text{Azimuth (antenna)}} \tag{20}$$

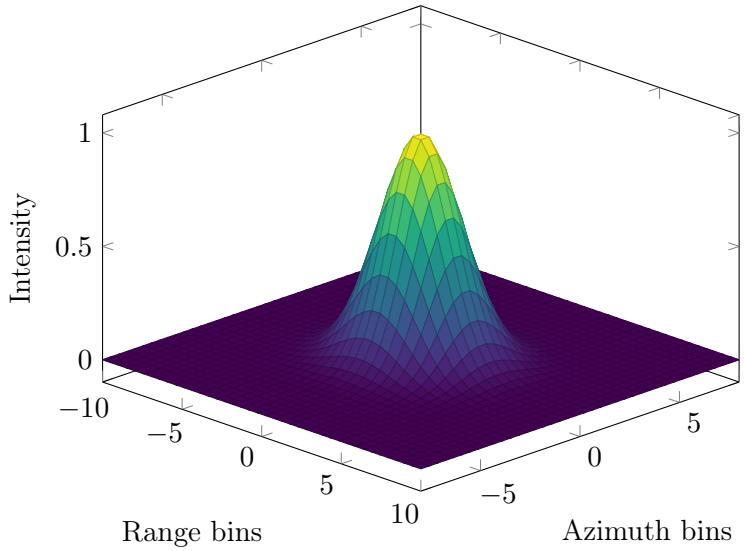

Figure 16: 2D radar Point Spread Function. The PSF is narrower in range (from pulse compression) and wider in azimuth (from beamwidth).

7.3 Polar to Cartesian Conversion

Finally, we convert from radar coordinates (R, ϕ) to image coordinates (x, y):

$$x = R\sin(\phi) \tag{21}$$

$$y = R\cos(\phi) \tag{22}$$

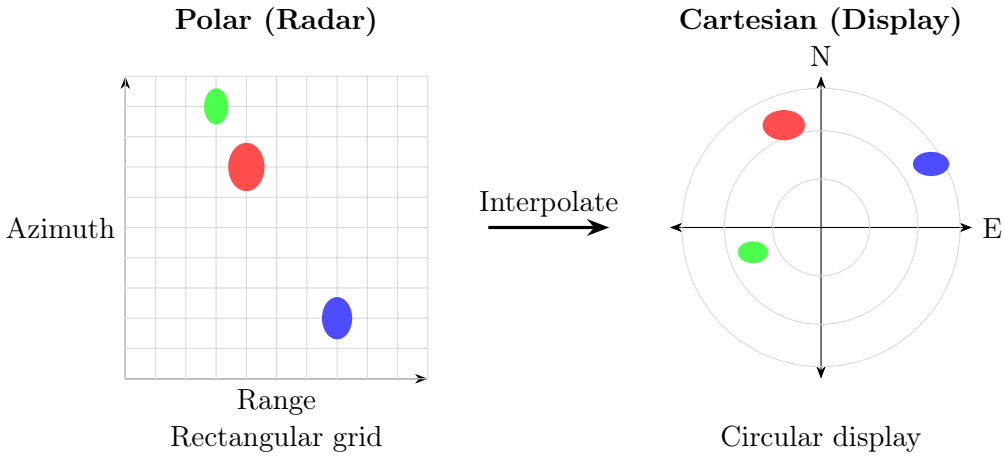

Figure 17: Polar to Cartesian scan conversion. Bilinear interpolation fills gaps in the Cartesian grid.

8 Complete Signal Flow Example

Let's trace a single target through the entire simulation:

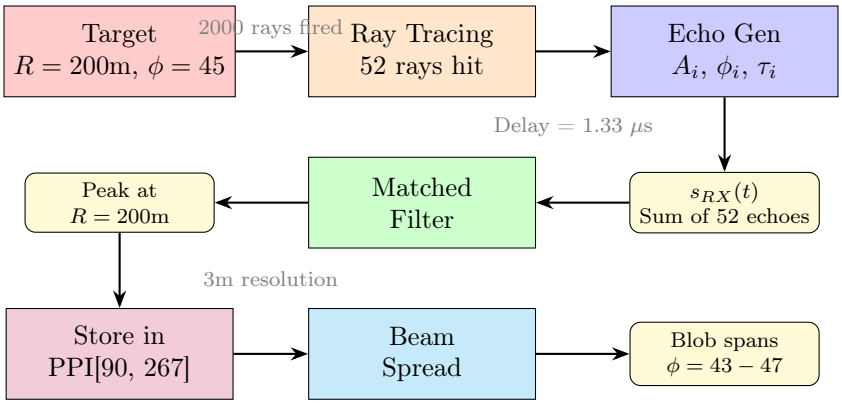

Figure 18: Complete signal flow for a single target at 200m range, 45° azimuth.

8.1 Numerical Example

For a target at $R = 200$ m, $\phi = 45$:

1. **Delay:** $\tau = 2R/c = 2 \times 200/(3 \times 10^8) = 1.33$ μs $= 267$ samples at 200 MSPS
2. **Phase:** $\phi = 4\pi f_0 R/c = 4\pi \times 9.41 \times 10^9 \times 200/(3 \times 10^8) = 78,873$ rad $= 12,553$ cycles
3. **Antenna Gain:** If ray is 1° off boresight: $G = \text{sinc}^2(2.783 \times 1/3.9) = 0.67$ (one-way)
4. **Two-way:** $G_{2way} = 0.67^4 = 0.20$ (-7 dB)
5. **Range Bin:** After compression, peak appears at bin 267×0.75m ≈ 200m
6. **Azimuth Bin:** $45/0.5 = 90$th bin

9 Summary

Stage	**Key Physics**
3D World	Triangle meshes, Möller-Trumbore intersection
Ray Tracing	Monte Carlo sampling within antenna beam
Echo Generation	$A \cdot e^{j\phi} \cdot s_{TX}$, includes path loss, multipath, atmosphere
Pulse Compression	FFT correlation, sinc response, windowing for sidelobes
Beam Spreading	Gaussian convolution matching beamwidth
PSF	2D spreading in range and azimuth
Scan Conversion	Bilinear interpolation, polar to Cartesian

Table 2: Summary of physics at each simulation stage